One-step construction of the multiple-qubit Rydberg controlled-PHASE gate

S. L. Su,[1,*] H. Z. Shen,[2,†] Erjun Liang,[1] and Shou Zhang[3,4]
[1]*School of Physics and Engineering, Zhengzhou University, Zhengzhou 450001, China*
[2]*Center for Quantum Sciences and School of Physics, Northeast Normal University, Changchun 130024, China*
[3]*Department of Physics, Yanbian University, Yanji, Jilin 133002, China*
[4]*Department of Physics, Harbin Institute of Technology, Harbin 150001, China*

(Received 11 February 2018; published 6 September 2018)

Although the three-body Rydberg antiblockade regime (RABR) can produce Rabi oscillation between the Rydberg collective excited state and the collective ground state, it is still hard to use the RABR to construct the three-qubit quantum logic gate in one step since the effective Hamiltonian is always accompanied by undesired Stark shifts. In order to overcome this difficulty, an additional laser is introduced to eliminate the Stark shifts in the ground-state subspace. And the initial RABR condition is modified to eliminate the remaining undesired Stark shifts in the collective-excitation subspace. The modified RABR is then generalized to the n ($n > 3$)-qubit case. Based on the proposed regime, one-step schemes to construct three- and n-qubit quantum controlled-PHASE gates are proposed without the requirement of atomic addressability. The asymmetric Rydberg-Rydberg interaction, which is more practical for Rydberg atoms, is also discussed and proven to be feasible for the modified RABR and quantum controlled-PHASE gate in theory. A full-Hamiltonian-based master equation is used to evaluate the performance and some experimental parameters are also considered.

DOI: 10.1103/PhysRevA.98.032306

I. INTRODUCTION

Neutral atoms have garnered much interest in the quantum information field due to advances in their experimental operation, especially in trapping and cooling. Rydberg atoms, neutral atoms that are excited to high-lying Rydberg states, exhibit large dipole moments when they are close enough [1,2]. This large-dipole-moment-induced interaction is called the Rydberg-Rydberg interaction (RRI). The RRI has been directly measured in experiments [3]. One of the interesting phenomena caused by RRI is Rydberg blockade, i.e., a frequency-matched classical laser field cannot excite both atoms at the same time [4,5] if the line width of the excitation is significantly narrower than the energy shift caused by the RRI, which has been observed in experiments between two Rydberg atoms located about 10 μm [6] apart through sequential driving and 4 μm [7] apart by collective driving, respectively. Via the contactless RRI, the photonic nonlinear dynamics is obtained in experiments [8]. Besides, the conditional dynamics of two Rydberg atoms can be easily achieved via RRI-induced energy shift [9], phase shift [10], blockade [11–18], Rydberg dressing [19–23], generalized Rabi frequency [24], or two-atom dark state [25]. Some of the above schemes are based on Förster-resonance-induced dipole-dipole interactions, which have been well studied for Rb-Rb and Cs-Cs with different atomic species [26].

In addition to the two-qubit conditional dynamics, multiple-qubit quantum logic gates, which perform a logic operation on a single target qubit depending on the state of the remaining control qubits, are also meaningful for the quantum algorithm [27–30] and quantum error correction [31,32]. The multiple-qubit logic gate can be decomposed into single- and two-qubit gates [29,33,34]. However, with an increasing number of qubits, the required number of single- and two-qubit quantum gates increases dramatically, which means that construction of the multiple-qubit gate directly is worth studying [35]. Based on the Rydberg blockade several schemes are proposed to construct multiple-qubit Rydberg quantum logic gates via exciting atoms into different Rydberg states [36], considering asymmetric Rydberg interactions [37,38], and sequent-driving-based Rydberg collective excitation [39]. With atomic addressability technology these schemes can maintain high fidelities through many operation steps.

Different from Rydberg blockade, a Rydberg antiblockade regime (RABR), which allows more than one Rydberg atom to be excited, was initially predicted by Ates *et al.* in an ultracold Rydberg gas [40] via a two-step excitation process. Then the predicated phenomenon was observed by Amthor *et al.* in experiments [41]. In addition, Pohl *et al.* found that, for three Rydberg atoms, the system would undergo the RABR once the dark state containing three excited Rydberg states was populated [42]. Following the work in Ref. [42], Qian *et al.* showed that the two-atom RABR can occur when they are interacting with a zero-area phase-jump pulse [43]. Then Zuo *et al.* [44] and Lee *et al.* [45] gave a strict condition for achieving effective Rabi oscillation between the collective Rydberg excited state and the ground state, in which detuning of the laser coupling was used to compensate the RRI energy [44–46]. Nevertheless, construction of the quantum gate was still not easy because undesired Stark shifts emerge [47,48]. On the other hand, Carr and Saffman proposed an interesting

*slsu@zzu.edu.cn
†shenhz458@nenu.edu.cn

scheme [49] to prepare entanglement via combination of the dissipative dynamics and the RABR, which pioneered a new method for preparation of the quantum entangled state in Rydberg atoms, and this was followed by a series of works [50].

In this paper, first, the conventional two-body RABR [44–50] is generalized to the three-body case via high-order perturbation theory. Then an additional laser is introduced to eliminate the undesired Stark shifts in the ground-state subspace. And the remaining undesired Stark shifts in the high-excitation subspace can also be entirely eliminated by modifying the RABR condition without adding any extra controls. The modified RABR is then generalized to the n ($n > 3$)-body case, based on which the multiple-qubit quantum controlled-PHASE gate is constructed in theory. In contrast to the other Rydberg multiple-qubit quantum logic gate, the present one can be implemented in one step and has no requirement regarding atom addressability for the symmetric RRI.

The rest of the paper is organized as follows. In Sec. II, the basic model, including the energy level and laser driving of the Rydberg atom (Sec. II A) and the many-body RABR (Sec. II B), is illustrated and analyzed. In Sec. III, the many-body RABR is modified and used to construct the controlled-PHASE gate. In addition, the asymmetric RRI and other practical situations are also discussed. The conclusion is given in Sec. IV.

II. BASIC MODEL

A. Energy level and laser driving

As shown in Fig. 1, we consider several trapped identical Rydberg atoms interacting with two laser pulses. The relevant energy level of the Rydberg atoms is shown in Fig. 1(c). The Rydberg state $|R\rangle$ is coupled to state $|1\rangle$ dispersively with blue detuning $-\Delta$ and Rabi frequency Ω, and the auxiliary state $|a\rangle$ is coupled to state $|1\rangle$ dispersively with red detuning δ and Rabi frequency ω.

In the interaction picture, the Hamiltonian of the n-atom system is $\hat{H} = \hat{H}_a + \hat{H}_v$, where

$$\hat{H}_a = \sum_{j=1}^{n} \frac{\Omega}{2}|1\rangle_j\langle R|e^{i\Delta t} + \frac{\omega}{2}|a\rangle_j\langle 1|e^{i\delta t} + \text{H.c.} \qquad (1)$$

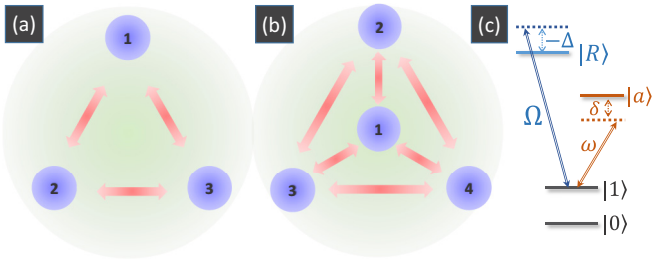

FIG. 1. Schematic of the many-body RABR and the multiple-qubit controlled-PHASE gate. (a) Three-qubit case. (b) Four-qubit case. (c) Energy level and the corresponding laser couplings for each Rydberg atom. $|0\rangle$ and $|1\rangle$ are two ground states that were used to encode the quantum information. $|R\rangle$ denotes the high-lying Rydberg state, and $|a\rangle$ denotes the ordinary auxiliary state. Ω (ω) is the Rabi frequency of the transition $|1\rangle \leftrightarrow |R(a)\rangle$ with the detuning $-\Delta(\delta)$.

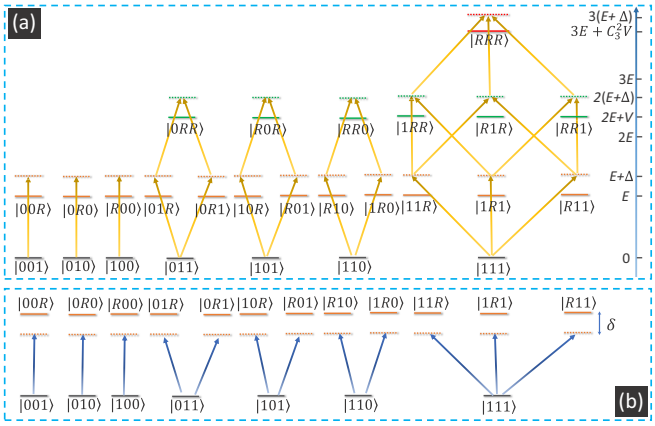

FIG. 2. Energy level diagram and dynamic processes of the Hamiltonian relevant to Ω as well as RRIs (a) and ω (b) in the three-atom basis. The states cannot be excited to the high-excitation subspace except for $|111\rangle$, due to the antiblockade regime. Nevertheless, Stark shifts would be obtained for these states due to the second-order perturbation theory. E denotes the energy of the Rydberg state in a single atom;V denotes the RRI strength. Δ and δ are laser detunings.

denotes the interactions between laser pulses and Rydberg atoms and

$$\hat{H}_v = \sum_{j=1}^{n-1}\sum_{k=2}^{n} V_{jk}|RR\rangle_{jk}\langle RR| \quad (j < k) \qquad (2)$$

denotes the RRI terms. In order to facilitate the analysis, without loss of generality, we set $V_{jk} = V$ for different atoms. For clearness, we first describe how to achieve the RABR based on a laser with Rabi frequency Ω and then show how to construct the quantum logic gate via the modified RABR, which relies on the transition from $|1\rangle$ to $|a\rangle$ induced by an auxiliary laser with Rabi frequency ω.

B. Rydberg antiblockade regime

1. Illustration of the dynamic process

In Fig. 2(a), we plot the energy level diagram of all the three-atom bases coupled to the the ground-state subspace ($|000\rangle$ is not considered since it is decoupled from the excitation process). Before discussing the n-body RABR, we first explain the dynamics process in Fig. 2(a) according to the different-excitation-number subspace as follows.

i. For the single-excitation subspace (the three-atom basis which contains one Rydberg state), the energy of the laser is $E + \Delta$ and that of the atomic transition from the zero- to the single-excitation subspace is E [see Fig. 2(a)]. It is obvious that the laser is detuned by Δ. We set the energy of the ground state (zero-excitation) subspace to 0 for simplicity.

ii. For the two-excitation subspace (the three-atom basis which contains two Rydberg states), the energy of the three-atom states is $2E + V$, which is shifted by the amount V due to the RRI. And the total energy of the two lasers is $2(E + \Delta)$. In this case, the laser is detuned with the state transition process from the zero- to the two-excitation subspace by the amount $2\Delta - V$.

iii. For the three-excitation subspace (the three-atom basis which contains three Rydberg states), the total energy of the laser is $3(E+\Delta)$ [see Fig. 2(a)]. And the energy of state $|RRR\rangle$ is $3E+C_3^2V$ [see Fig. 2(a)], in which $3E$ originates from the excited energy levels and C_3^2V is induced by the two-body RRIs (here 3 denotes three atoms and 2 means that RRI is the two-body interaction). In this case, the laser is detuned with the state transition process from $|111\rangle$ to the three-excitation state $|RRR\rangle$ by the amount $3\Delta-C_3^2V$.

To explain why the energy shifts in the two- and three-excitation subspaces are V and C_3^2V, respectively, we rewrite the RRI Hamiltonian in the three-atom basis as

$$\begin{aligned}\hat{H}_v &= V|R\rangle_1\langle R|\otimes|R\rangle_2\langle R|\otimes\hat{\mathcal{I}}_3+V|R\rangle_1\langle R|\otimes\hat{\mathcal{I}}_2\\ &\quad\otimes|R\rangle_3\langle R|+V|\otimes\hat{\mathcal{I}}_1\otimes|R\rangle_2\langle R|\otimes|R\rangle_3\langle R|\\ &\equiv V\sum_{k=1}^{6}\hat{\mathcal{O}}_k+C_3^2V|RRR\rangle\langle RRR|,\end{aligned}\tag{3}$$

in which $\hat{\mathcal{O}}_k$ denotes the kth operator of the set $\{|RR0\rangle\langle RR0|,\ |RR1\rangle\langle RR1|,\ |R0R\rangle\langle R0R|,\ |R1R\rangle\langle R1R|,\ |0RR\rangle\langle 0RR|,\ |1RR\rangle\langle 1RR|\}$. The terms $V\sum_{k=1}^{6}\hat{\mathcal{O}}_k$ and $C_3^2V|RRR\rangle\langle RRR|$ in Eq. (3) correspond to the two- and three-excitation subspaces, respectively, as shown in Fig. 2(a).

2. *N-body Rydberg antiblockade regime*

The basic mechanism behind Rydberg blockade is that the Rydberg energy level is shifted due to the RRI. Thus, the key to achieve antiblockade is to use dispersive lasers to compensate the energy shift. In other words, strictly equivalent relations should be built between the laser energy and the atomic transition energy after considering the RRI.

For the three-body case, as mentioned above, the effective detuning between the laser driving and the state transition from the single- to the three-excitation subspace is $3\Delta-C_3^2V$. Thus, if one sets $3\Delta-C_3^2V=0$, i.e., $\Delta=V$, the transition process $|111\rangle\rightarrow|RRR\rangle$ will be resonant [see Fig. 2(a)].

For the n-body case, the energy of the n-excitation state is $nE+C_n^2V$, while the total energy of the laser is $nE+n\Delta$. Therefore, if the condition

$$C_n^2V-n\Delta=0\tag{4}$$

is satisfied, the laser driving process will be resonant with the atomic transition process from the ground-state subspace to the n-excitation subspace. Therefore, Eq. (4) is the n-body RABR condition.

III. ONE-STEP CONSTRUCTION OF THE CONTROLLED-PHASE GATE

A. Dynamical description

Suppose the dispersive condition $\Delta\gg\Omega/2$ is satisfied; under the three-body RABR the initial states in the computation subspace cannot be excited to the high-excitation subspace except $|111\rangle$. The corresponding dynamic processes associated with Ω and RRI are shown in Fig. 2(a) and illustrated in Sec. II B 1.

To get the three-qubit controlled-PHASE gate, the system Hamiltonian with the concise form $\hat{H}=\lambda(|111\rangle\langle RRR|+\text{H.c.})$ is completely feasible, in which λ is the effective coupling strength. However, from the dynamic process shown in Fig. 2(a) and the Appendix, one can get the effective Hamiltonian related to Ω and RRI as

$$\begin{aligned}\hat{H}_{\text{eff}}^{\Omega}&=\frac{3\Omega^3}{4\Delta^2}(|111\rangle\langle RRR|+\text{H.c.})\\&\quad+\frac{3\Omega^2}{4\Delta}|RRR\rangle\langle RRR|+\sum_j(m\Omega^2/4\Delta)\hat{\mathcal{S}}_j,\end{aligned}\tag{5}$$

where $(\Omega^2/4\Delta)\hat{\mathcal{S}}$ denotes the Stark shift of three-atom states in the ground-state subspace and m denotes the number of $|1\rangle$ in the three-atom basis made up of $\hat{\mathcal{S}}_j$. The Stark shifts complicate the system's unitary dynamics and interfere with the desired transition process between $|111\rangle$ and $|RRR\rangle$. Thus, we are most interested in completely eliminating $\hat{\mathcal{S}}$.

B. Modified Rydberg antiblockade regime

1. *Three-body case*

To eliminate $\hat{\mathcal{S}}$, we introduce an additional laser that couples $|1\rangle$ to the ordinarily auxiliary state $|a\rangle$ with Rabi frequency ω and detuning δ. If the dispersive condition $\delta\gg\omega/2$ is satisfied, $|1\rangle$ cannot be excited to auxiliary state $|a\rangle$, while Stark shifts will be generated. Under the condition $|\Delta+\delta|\gg|\Omega\omega/(4\bar{\Delta})|$ with $1/\bar{\Delta}=(-1/\Delta+1/\delta)/2$, the Raman process $|R\rangle\leftrightarrow|a\rangle$ mediated by $|1\rangle$ is inhibited. Thus, we can consider the effective Hamiltonians induced by Ω and ω independently.

Based on the second-order perturbation theory, one can get the effective Hamiltonian relevant to ω as [see Fig. 2(b) and the Appendix]:

$$\hat{H}_{\text{eff}}^{\omega}=-\sum_j(m\omega^2/4\delta)\hat{\mathcal{S}}_j.\tag{6}$$

If the condition

$$\Omega^2/\Delta=\omega^2/\delta\tag{7}$$

is satisfied, Eq. (6) and the last term in Eq. (5) cancel each other out. Then the effective Hamiltonian of the whole system will be

$$\hat{H}_{\text{eff}}=\frac{3\Omega^3}{4\Delta^2}(|111\rangle\langle RRR|+\text{H.c.})+\frac{3\Omega^2}{4\Delta}|RRR\rangle\langle RRR|.\tag{8}$$

Equation (8) is still not efficient to construct a three-qubit quantum logic gate since there is still one Stark-shift term in the three-excitation subspace.

As mentioned above, the RRI terms $V|RR\rangle_{12}\langle RR|+V|RR\rangle_{13}\langle RR|+V|RR\rangle_{23}\langle RR|$ generate $3V|RRR\rangle\langle RRR|$ under the three-atom basis. Therefore, if the RRI strength V in the initial Hamiltonian is decreased by the amount $\Omega^2/(4\Delta)$, i.e.,

$$V=\Delta-\Omega^2/4\Delta,\tag{9}$$

the effective Hamiltonian, Eq. (8), will add an extra term, $-3\Omega^2/4\Delta|RRR\rangle\langle RRR|$, and further be simplified to

$$\hat{H}_{\rm eff} = \frac{3\Omega^3}{4\Delta^2}(|111\rangle\langle RRR| + \text{H.c.}), \tag{10}$$

based on which the three-qubit quantum controlled-PHASE gate $\hat{U} = e^{i\pi|111\rangle\langle 111|}$ can be achieved at time $t = 4\pi\Delta^2/(3\Omega^3)$ in one step.

2. N-body case

The three-body RABR can be extended to the n ($n > 3$)-body case and further be used to construct an n-qubit ($n > 3$) quantum controlled-PHASE gate through high-order perturbation theory. Through simple but extended calculations similar to that in the Appendix, one can get the n-qubit effective Hamiltonian,

$$\hat{H}_{\rm eff} = \frac{A_n^n\Omega^n}{2^n\Delta^{n-1}}\Big(|\underbrace{11\ldots1}_{n}\rangle\langle\underbrace{RR\ldots R}_{n}| + \text{H.c.}\Big) + \frac{A_n^1\Omega^2}{4\Delta}|\underbrace{RR\ldots R}_{n}\rangle\langle\underbrace{RR\ldots R}_{n}|, \tag{11}$$

with the n-body RABR condition $\Delta = C_n^2 V/n$ and the condition in Eq. (7). In Eq. (11), $\Omega^n/(2^n\Delta^{n-1})$ is generated by the nth-order perturbation theory and A_n^n is the result of the permutation and combination of all possible transition paths from $|11\ldots1\rangle$ to $|RR\ldots R\rangle$. $\Omega^2/4\Delta$ is produced by the second-order perturbation theory when $|RR\ldots R\rangle$ couples to the $n-1$ Rydberg-excitation subspace, and A_n^1 denotes the number of all possible coupling paths. Then one can get the effective Hamiltonian

$$\hat{H}_{\rm eff} = \frac{A_n^n\Omega^n}{2^n\Delta^{n-1}}\Big(|\underbrace{11\ldots1}_{n}\rangle\langle\underbrace{RR\ldots R}_{n}| + \text{H.c.}\Big), \tag{12}$$

with the modified n-body RABR condition

$$V = n\Delta/C_n^2 - A_n^1\Omega^2/(4C_n^2\Delta). \tag{13}$$

The first term on the right-hand side of Eq. (13) denotes the conventional n-body RABR in Eq. (4), and the second term on the right-hand side of Eq. (13) is introduced to eliminate the last term in Eq. (11). C_n^2 is the number of two-body RRI terms among n Rydberg atoms that contributes to $|RR\ldots R\rangle\langle RR\ldots R|$. With Eq. (12), the n-qubit controlled-PHASE gate $\hat{U} = e^{i\pi|11\ldots1\rangle\langle 11\ldots1|}$ can be constructed at time $t = 2^n\pi\Delta^{n-1}/(A_n^n\Omega^n)$ in one step.

Although the schemes for realizing the n-qubit ($n \geq 3$) controlled-PHASE gate that have been proposed [36–38] individually address Rydberg atoms, the existence of the present scheme is still necessary since (i) it can be implemented in one step regardless of the qubit number of the quantum controlled-PHASE gate, (ii) it has no requirement for atomic addressability under the symmetric RRI, and (iii) it is based on the modified many-body RABR.

C. Analysis and discussion of the gate

1. Dynamics consistency

The effective dynamics, based on which we choose the system parameters, is achieved by the perturbation theory. Thus the feasibility and validity of the effective dynamics should be analyzed. In Figs. 3(a) and 3(b), we plot the evolution fidelities of three- and four-qubit quantum controlled-PHASE gates under effective and full Hamiltonians, respectively. The results show that the full and effective dynamics bear a higher level of consistency.

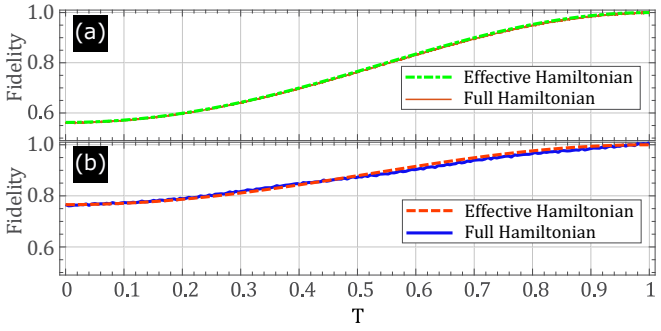

FIG. 3. Fidelities of the quantum controlled-PHASE gate plotted with the full [Eqs. (1) plus (2)] and effective [Eq. (12)] Hamiltonians. (a) Three-qubit case. (b) Four-qubit case. In (a), the dot-dashed green line denotes the effective-Hamiltonian-based result, and the solid saffron yellow line denotes the full-Hamiltonian-based result. In (b), the dashed red line denotes the effective-Hamiltonian-based result, and the solid blue line denotes the full-Hamiltonian-based result. The initial state is set as $\sum_{i=1}^{n}\otimes(|0\rangle + |1\rangle)_i/\sqrt{2}$. The final states given by the ideal and practical controlled-PHASE gate, respectively, are used to plot the fidelity. The parameters are chosen as $n = 3$, $\Delta/\Omega = 12$, $\omega/\Omega = 3.25$, and $\gamma = 0$ in (a) and $n = 4$, $\Delta/\Omega = 10.6$, $\omega/\Omega = 3.8$, and $\gamma = 0$ in (b).

2. Average fidelity

One can use the mean value of fidelities corresponding to several groups of random initial states to define the average fidelity

$$\overline{F} = \frac{1}{k}\sum_{m=1}^{k}\left[\text{Tr}\sqrt{\sqrt{\hat{\rho}_m^{\rm ideal}}\hat{\rho}_m(t)\sqrt{\hat{\rho}_m^{\rm ideal}}}\right]^2, \tag{14}$$

where $\rho_m(t)$ denotes the practical output density matrix corresponding to the random mth input state, and $\hat{\rho}_m^{\rm ideal}$ is the corresponding matrix obtained from the ideal controlled-PHASE gate. Alternatively, we define another average fidelity [47],

$$\overline{F} = \frac{1}{2\pi}\int_0^{2\pi} d\eta\langle\psi_{\rm ideal}|\hat{\rho}(t)|\psi_{\rm ideal}\rangle, \tag{15}$$

in which η is the parameter of the initial state. $\hat{\rho}(t)$ is the practically final density matrix obtained by solving the master equation. $|\psi_{\rm ideal}\rangle$ is the final state obtained by the ideal quantum controlled-PHASE gate.

In Figs. 4(a) and 4(b), we use the random-initial-state method defined in Eq. (14) and the integral method defined in Eq. (15) to evaluate the fidelities, respectively. Figure 4 shows that the scheme may have a fidelity of more than 0.98 since $\gamma/\Omega \sim 10^{-4}$ is not hard to achieve in experiments due to the long lifetime of the Rydberg energy level [51].

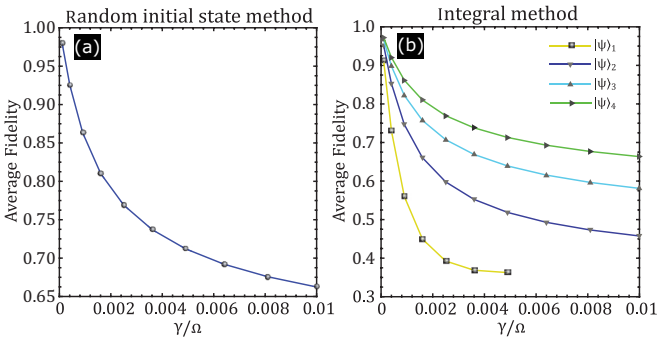

FIG. 4. Average fidelities of the three-qubit controlled-PHASE gate versus γ. (a) Random-initial-state method. (b) Integral method. For simplicity, we set $|\psi\rangle_1 = \sin\eta(|000\rangle + |001\rangle + |010\rangle + |011\rangle + |100\rangle + |101\rangle + |110\rangle)/\sqrt{7} + \cos\eta|111\rangle$, $|\psi\rangle_2 = \sin\eta(|000\rangle + |001\rangle + |010\rangle + |011\rangle + |100\rangle + |101\rangle)/\sqrt{6} + \cos\eta(|110\rangle + |111\rangle)/\sqrt{2}$, $|\psi\rangle_3 = \sin\eta(|000\rangle + |001\rangle + |010\rangle + |011\rangle + |100\rangle)/\sqrt{5} + \cos\eta(|101\rangle + |110\rangle + |111\rangle)/\sqrt{3}$, and $|\psi\rangle_4 = \sin\eta(|000\rangle + |001\rangle + |010\rangle + |011\rangle)/2 + \cos\eta(|100\rangle + |101\rangle + |110\rangle + |111\rangle)/2$. The parameters are chosen as $\Delta/\Omega = 12$, $\omega/\Omega = 3.25$; γ/Ω ranges from 10^{-4} to 10^{-2}. δ is chosen based on Eq. (7).

3. *Asymmetric Rydberg interaction*

Here, we consider how to construct a controlled-PHASE gate under asymmetric RRI, which extends the scheme to a more general case. We take the three-qubit case as an example to illustrate the process.

As shown in Fig. 1(a), suppose the RRI strengths between atom j and atom k, V_{jk}, do not equal each other. The energy of the three-excitation state $|RRR\rangle$ is then changed from $3E + C_3^2 V$ to $3E + V_{12} + V_{13} + V_{23}$ [similar to the analytic process used to get Eq. (3)]. To simplify the perturbation-theory-based effective dynamics, we set the Rabi frequencies (Ω) relevant to the process $|1\rangle \to |R\rangle$ of all the atoms the same, while the corresponding detuning is Δ_i for the ith atom. Consequently, the total energy of the laser is $3E + \sum_{i=1}^{3}\Delta_i$. Then, if the condition

$$3E + V_{12} + V_{13} + V_{23} - \left(3E + \sum_{i=1}^{3}\Delta_i\right) = 0 \tag{16}$$

is satisfied, the three-body RABR is achieved for asymmetric RRIs. Similarly to the process used to get Eq. (5), under the large-detuning condition, one can get the effective Hamiltonian relevant to Ω as [52]

$$\hat{H}_{\rm eff}^{\Omega} = \Omega_{\rm eff}(|111\rangle\langle RRR| + \text{H.c.}) + \hat{\mathcal{P}}_1 + \hat{\mathcal{P}}_2, \tag{17}$$

in which

$$\Omega_{\rm eff} = \frac{\Omega^3}{8}\left[\frac{\Delta_1+\Delta_2}{\Delta_1\Delta_2(V_{13}+V_{23}-\Delta_3)} + \frac{\Delta_1+\Delta_3}{\Delta_1\Delta_3(V_{12}+V_{23}-\Delta_2)} + \frac{\Delta_2+\Delta_3}{\Delta_2\Delta_3(V_{12}+V_{13}-\Delta_1)}\right], \tag{18}$$

$$\hat{\mathcal{P}}_1 = \frac{\Omega^2}{4}\left(\frac{1}{V_{13}+V_{23}-\Delta_3} + \frac{1}{V_{12}+V_{23}-\Delta_2} + \frac{1}{V_{12}+V_{13}-\Delta_1}\right)|RRR\rangle\langle RRR|, \tag{19}$$

and

$$\begin{aligned}\hat{\mathcal{P}}_2 = {} & \Omega^2/(4\Delta_1)|100\rangle\langle 100| + \Omega^2/(4\Delta_2)|010\rangle\langle 010| + \Omega^2/(4\Delta_3)|001\rangle\langle 001| + [\Omega^2/(4\Delta_2) + \Omega^2/(4\Delta_3)]|011\rangle\langle 011| \\ & + [\Omega^2/(4\Delta_1) + \Omega^2/(4\Delta_2)]|110\rangle\langle 110| + [\Omega^2/(4\Delta_1) + \Omega^2/(4\Delta_3)]|101\rangle\langle 101|.\end{aligned} \tag{20}$$

The term $\hat{\mathcal{P}}_2$ in Eq. (17) can be eliminated by considering the auxiliary transition $|1\rangle \to |a\rangle$. Differently from the symmetric-RRI-based scheme, for the auxiliary transition we set the detuning of the ith atom to δ_i, while the Rabi frequencies ω for different atoms are the same. Then, under the large-detuning condition, the effective Hamiltonian relevant to ω is

$$\begin{aligned}\hat{H}_{\rm eff}^{\omega} = {} & -\omega^2/(4\delta_1)|100\rangle\langle 100| - \omega^2/(4\delta_2)|010\rangle\langle 010| - \omega^2/(4\delta_3)|001\rangle\langle 001| - [\omega^2/(4\delta_2) + \omega^2/(4\delta_3)]|011\rangle\langle 011| \\ & - [\omega^2/(4\delta_1) + \omega^2/(4\delta_2)]|110\rangle\langle 110| - [\omega^2/(4\delta_1) + \omega^2/(4\delta_3)]|101\rangle\langle 101|.\end{aligned} \tag{21}$$

It is easy to see that if

$$\Omega^2/(4\Delta_j) = \omega^2/(4\delta_j) \tag{22}$$

is satisfied, the full effective Hamiltonian is changed to

$$\hat{H}_{\rm eff} = \hat{H}_{\rm eff}^{\Omega} + \hat{H}_{\rm eff}^{\omega} = \Omega_{\rm eff}(|111\rangle\langle RRR| + \text{H.c.}) + \hat{\mathcal{P}}_1. \tag{23}$$

$\hat{\mathcal{P}}_1$ can also be eliminated by modifying the antiblockade condition, (16); before this we set $\Delta_1 = V_{23}$, $\Delta_2 = V_{13}$, $\Delta_3 = V_{12}$ without loss of generality. [It should be noted that there are many choices for the relations between RRI and detuning that fulfill Eq. (16); we just use this set of parameters to verify the feasibility of the scheme.] To eliminate $\hat{\mathcal{P}}_1$, we reset

$$\begin{aligned} V_{12} &= \Delta_3 - \frac{\Omega^2}{4(V_{13}+V_{23}-\Delta_3)}, \\ V_{23} &= \Delta_1 - \frac{\Omega^2}{4(V_{12}+V_{13}-\Delta_1)}, \\ V_{13} &= \Delta_2 - \frac{\Omega^2}{4(V_{12}+V_{23}-\Delta_2)}. \end{aligned} \tag{24}$$

One can see clearly how the added terms in Eq. (24) cancel $\hat{\mathcal{P}}_1$ if the RRIs are rewritten in the three-atom basis.

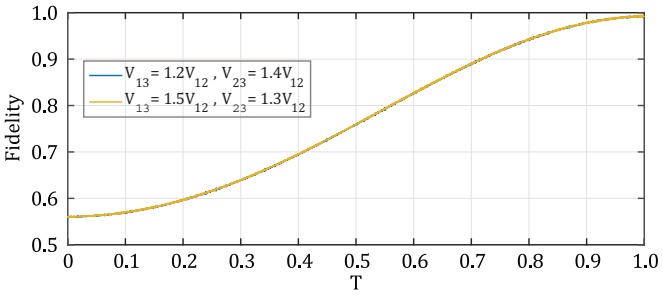

FIG. 5. Fidelities of the three-qubit controlled-PHASE gate in one evolution period with two groups of asymmetric Rydberg parameters. The initial and final states are the same as those in Fig. 3 and the full Hamiltonian is used for numerical simulation. The parameters are chosen as $V_{12}/\Omega = 10$, $\omega/\Omega = 3.25$. Δ_i and δ_i are chosen based on Eqs. (24) and (22), respectively.

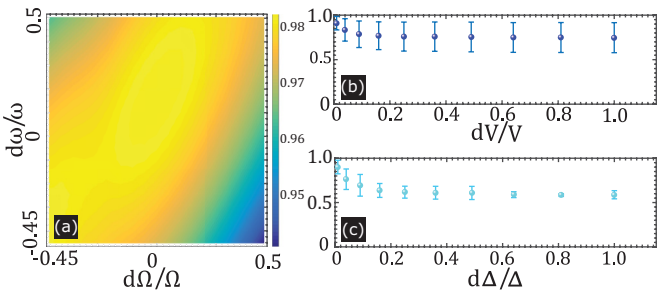

FIG. 6. Fidelity of the quantum controlled-PHASE gate with variation of parameters for symmetric RRI. All coordinate values are percentages. For (b) and (c), 100 groups of parameters that satisfy the Gauss distribution are considered for one deviation point of the parameters. Here we use one specific initial state, $\sum_{i=1}^{3}\otimes[(|0\rangle + |1\rangle)_i/\sqrt{2}]$, and the corresponding final state to simulate the fidelity. The parameters are chosen as $\Delta/\Omega = 12$, $\omega/\Omega = 3.25$, and $\gamma/\Omega = 10^{-4}$. δ is chosen based on Eq. (7).

Then the effective Hamiltonian of the whole system is changed to

$$\hat{H}_{\text{eff}} = \Omega_{\text{eff}}(|111\rangle\langle RRR| + \text{H.c.}), \tag{25}$$

which can be used to construct the quantum controlled-PHASE gate in one step. In Fig. 5, the fidelities of the scheme with two groups of asymmetric RRIs are plotted in one evolution period, which means the scheme can be implemented over a wider range of systematic parameters on the premise that the atomic addressability is provided.

4. Experimental considerations

Experimentally, a two-photon process to excite the ground state to the Rydberg state has been demonstrated in Refs. [6,7,12,53]; π polarized 780- and 480-nm beams are tuned for resonant excitation from the ground state, $5s_{1/2}$, $F = 2$, to the Rydberg state, $97d_{5/2}$, $m_j = 5/2$, with an effective Rabi frequency $\Omega/2\pi = 0.67$ MHz, and the atomic decay rate of the Rydberg state is about $2\pi \times 1$ kHz. The calculated RRI strength for Rydberg atoms separated by 10.2 μm is about $B/2\pi = 9.3$ MHz. In Ref. [53], Δ_p is set to $2\pi \times 2$ GHz, while in Ref. [12] it is $2\pi \times 1.1$ GHz. Thus, on one hand, the effective Rabi frequency can be varied by changing the detunings of the intermediate state Δ_p. On the other hand, very recently, coherent optical excitation to Rydberg states with an adjustable effective Ω ($\Omega_{\max} = 2\pi \times 10$ MHz) has also been demonstrated [54] through tuning of the Rabi frequency of the process that couples the ground state to the intermediate state.

Besides, a single-photon process is also realized for the Rydberg dressing scheme [55], which couples directly from the ground state, $6s_{1/2}$, $F = 4$, to the Rydberg level, $64p_{3/2}$, of ^{133}Cs atoms through use of a 319-nm laser.

Following the experiments in Refs. [12] and [53], for our model the energy level configuration can be chosen as $|0\rangle \equiv |5s_{1/2},\ F = 1,\ m = 0\rangle$, $|1\rangle \equiv |5s_{1/2},\ F = 2,\ m = 0\rangle$, and $|R\rangle \equiv |97d_{5/2}, m_j = 5/2\rangle$. If the atomic distance is set as 7.128 13 μm, the RRI strength will be $V/2\pi = 79.8417$ MHz. After varying the 790-nm laser power to five times higher than that in Ref. [12] and setting $\Delta_p/2\pi = 0.55$ GHz, $\Omega/2\pi = 6.7$ MHz is achieved. Besides, the resonant two-photon process should be adjusted to the dispersive process with detuning $\Delta = (V + \sqrt{V^2 + 4\Omega^2})/2 \cong 12\Omega$. Since state $|a\rangle$ is not in the computation subspace, we here use only the conditions relevant to ω and do not give the exact level configuration of $|a\rangle$ temporarily. The decay rate of $|a\rangle$ is supposed to be a magnitude greater than that of the $|R\rangle$ state, and $\omega = 3.25\Omega$ is used. Then, for the three-qubit case, $\overline{F} = 0.9603$ (integral method) and $\overline{F}_{\text{ran}} = 0.9679$ (random-initial-state method) are achieved, respectively. In addition, the single-photon process is feasible for our scheme.

5. Robustness to parameter variation

In the analysis above, we have assumed that the parameters were invariant during the operation process. However, the system instability and the operation inaccuracy may induce tiny variations in the system parameters. To evaluate their influence, we plot the fidelities versus the relative variation of parameters Ω, ω, Δ, and V in Fig. 6. The results show that the scheme has a good robustness to the variations of parameters Ω and ω. Nevertheless, the variation of V and Δ may have a certain influence since the RABR would be destroyed. However, this influence could be minimized with the use of the Rydberg dressing method [19–22] as well as the introduction of a Doppler-free configuration that involves counter-propagating lasers [19].

IV. CONCLUSION

In this paper, we first generalize the conventional two-body RABR to the many-body case. Then undesired Stark shifts in the many-body RABR are canceled out by (i) introducing an additional laser and (ii) modifying the many-body RABR condition. The well-designed many-body RABR is then used to construct the multiple-qubit controlled-PHASE gate in one step. We hope the proposed RABR and the multiple-qubit controlled-PHASE gate will find some applications in future Rydberg-atom-based quantum information processing tasks with the development of quantum technology.

ACKNOWLEDGMENTS

We would like to thank the anonymous referee for comments that help improve the representation and quality of the manuscript. We would also like to thank Dr. S. Xu for useful suggestions about the representation of the manuscript. S.L.S. would like to thank Dr. D.-Y. Wang for reexamination of the derivation process of the effective Hamiltonian in Method 1 of the Appendix. This work was supported by National Natural Science Foundation of China under Grants No. 11804308 and No. 11705025, and China Postdoctoral Science Foundation under Grants No. 2017T100192 and No. 2018T110735.

APPENDIX: DERIVATION OF THE EFFECTIVE HAMILTONIAN, (8)

1. Method 1

First, since the condition $\Omega\omega/(4\bar{\Delta}) \ll |\Delta+\delta|$ with $\bar{\Delta} = (2\Delta\delta)/(\Delta-\delta)$ is satisfied, the Raman transition process between state $|R\rangle$ and state $|a\rangle$ is inhibited. Thus, the effective Hamiltonian induced by dispersive lasers with Rabi frequencies Ω and ω can be considered independently. One can rewrite the terms in Hamiltonian (1) relevant to Ω with the three-atom basis as $\hat{H}_{a\Omega} = \hat{H}_{a\Omega1} + \hat{H}_{a\Omega2} + \hat{H}_{a\Omega3}$, in which

$$\begin{aligned}
\hat{H}_{a\Omega1} &= \frac{\Omega}{2}e^{i\Delta t}(|100\rangle\langle R00| + |101\rangle\langle R01| + |110\rangle\langle R10| \\
&\quad + |111\rangle\langle R11| + |010\rangle\langle 0R0| + |011\rangle\langle 0R1| \\
&\quad + |110\rangle\langle 1R0| + |111\rangle\langle 1R1| + |001\rangle\langle 00R| \\
&\quad + |011\rangle\langle 01R| + |101\rangle\langle 10R| + |111\rangle\langle 11R|) + \text{H.c.}, \\
\hat{H}_{a\Omega2} &= \frac{\Omega}{2}e^{i\Delta t}(|10R\rangle\langle R0R| + |11R\rangle\langle R1R| + |1R0\rangle\langle RR0| \\
&\quad + |1R1\rangle\langle RR1| + |01R\rangle\langle 0RR| + |11R\rangle\langle 1RR| \\
&\quad + |R10\rangle\langle RR0| + |R11\rangle\langle RR1| + |0R1\rangle\langle 0RR| \\
&\quad + |1R1\rangle\langle 1RR| + |R01\rangle\langle R0R| + |R11\rangle\langle R1R|) \\
&\quad + \text{H.c.}, \\
\hat{H}_{a\Omega3} &= \frac{\Omega}{2}e^{i\Delta t}(|1RR\rangle + |R1R\rangle + |RR1\rangle)\langle RRR| + \text{H.c.}
\end{aligned} \tag{A1}$$

Similarly, one can also rewrite $\hat{H}_v = \hat{H}_{v1} + \hat{H}_{v2}$, where

$$\begin{aligned}
\hat{H}_{v1} &= V(|RR0\rangle\langle RR0| + |R0R\rangle\langle R0R| + |0RR\rangle\langle 0RR| \\
&\quad + |RR1\rangle\langle RR1| + |R1R\rangle\langle R1R| + |1RR\rangle\langle 1RR|), \\
\hat{H}_{v2} &= 3V|RRR\rangle\langle RRR|.
\end{aligned} \tag{A2}$$

Before deriving the effective Hamiltonian, we move the Hamiltonian to the rotation frame with respect to $\hat{U} = e^{-i(\hat{H}_v+\hat{H}_0)t}$, in which

$$\begin{aligned}
\hat{H}_0 &= \Delta(|RR0\rangle\langle RR0| + |R0R\rangle\langle R0R| + |0RR\rangle\langle 0RR| \\
&\quad + |RR1\rangle\langle RR1| + |R1R\rangle\langle R1R| + |1RR\rangle\langle 1RR|).
\end{aligned} \tag{A3}$$

Thus, the full Hamiltonian can be reexpressed as $\hat{H} = \hat{H}_{a\Omega1} + \hat{H}'_{a\Omega2} + \hat{H}'_{a\Omega3} - \hat{H}_0$ with

$$\begin{aligned}
\hat{H}'_{a\Omega2} &= \frac{\Omega}{2}e^{-i\Delta t}(|10R\rangle\langle R0R| + |11R\rangle\langle R1R| + |1R0\rangle\langle RR0| \\
&\quad + |1R1\rangle\langle RR1| + |01R\rangle\langle 0RR| + |11R\rangle\langle 1RR| \\
&\quad + |R10\rangle\langle RR0| + |R11\rangle\langle RR1| + |0R1\rangle\langle 0RR| \\
&\quad + |1R1\rangle\langle 1RR| + |R01\rangle\langle R0R| + |R11\rangle\langle R1R|) + \text{H.c.}, \\
\hat{H}'_{a\Omega3} &= \frac{\Omega}{2}(|1RR\rangle + |R1R\rangle + |RR1\rangle)\langle RRR| + \text{H.c.}
\end{aligned} \tag{A4}$$

We use $\hat{P}^{(\prime)}(\pm\Delta)_{a\Omega j}(j = 1, 2, 3)$ to denote the terms of $\hat{H}^{(\prime)}_{a\Omega j}$ associated with $(\Omega/2)e^{\pm i\Delta t}$. Thus, the effective Hamiltonian among zero-, single-, and two-excitation subspaces can be achieved as [56]

$$\begin{aligned}
\hat{H}^{(0-2)}_{\text{eff}} &= \frac{\Omega^2}{4\Delta}\{[\hat{P}(\Delta)_{a\Omega1}, \hat{P}(-\Delta)_{a\Omega1} + \hat{P}'(-\Delta)_{a\Omega2}] \\
&\quad + [\hat{P}'(\Delta)_{a\Omega2}, \hat{P}(-\Delta)_{a\Omega1} + \hat{P}'(-\Delta)_{a\Omega2}]\} \\
&= \hat{H}^{(0-2)}_{\text{eff,part}} + \frac{\Omega^2}{2\Delta}\big[(|101\rangle\langle R0R| + |110\rangle\langle RR0| \\
&\quad + |011\rangle\langle 0RR|) + |111\rangle(\langle RR1| + \langle R1R| \\
&\quad + \langle 1RR|) + \text{H.c.}\big],
\end{aligned} \tag{A5}$$

where

$$\begin{aligned}
\hat{H}^{(0-2)}_{\text{eff,part}} &= \frac{\Omega^2}{4\Delta}\{|100\rangle\langle 100| + |010\rangle\langle 010| + |001\rangle\langle 001| \\
&\quad + 2(|110\rangle\langle 110| + |101\rangle\langle 101| + |011\rangle\langle 011|) \\
&\quad + 3|111\rangle\langle 111| - \big[|R00\rangle\langle R00| + |0R0\rangle\langle 0R0| \\
&\quad + |00R\rangle\langle 00R| + 2(|R01\rangle\langle R01| + |R10\rangle\langle R10| \\
&\quad + |0R1\rangle\langle 0R1| + |1R0\rangle\langle 1R0| + |01R\rangle\langle 01R| \\
&\quad + |10R\rangle\langle 10R|) \\
&\quad + 3(|R11\rangle\langle R11| + |1R1\rangle\langle 1R1| + |11R\rangle\langle 11R|)\big] \\
&\quad + 2(|RR0\rangle\langle RR0| + |RR1\rangle\langle RR1| + |R0R\rangle\langle R0R| \\
&\quad + |R1R\rangle\langle R1R| + |0RR\rangle\langle 0RR| + |1RR\rangle\langle 1RR|)\}.
\end{aligned}$$

Now, the whole Hamiltonian relevant to Ω and RRI is $\hat{H} = \hat{H}^{(0-2)}_{\text{eff}} + \hat{H}'_{a\Omega3} - \hat{H}_0$. We now move the whole Hamiltonian to the rotation frame with respect to $\hat{U} = e^{i\hat{H}_0 t}$ and get $\hat{H} =$

$\hat{H}_{\rm eff}^{(0-2)'}+\hat{H}''_{a\Omega 3}$, in which

$$\begin{aligned}\hat{H}_{\rm eff}^{(0-2)'} &= \hat{H}_{\rm eff,part}^{(0-2)}+\frac{\Omega^2}{2\Delta}[(|101\rangle\langle R0R|+|110\rangle\langle RR0|\\ &\quad+|011\rangle\langle 0RR|)e^{i\Delta t}+|111\rangle(\langle RR1|+\langle R1R|\\ &\quad+\langle 1RR|)e^{i\Delta t}+\text{H.c.}],\\ \hat{H}''_{a\Omega 3} &= \frac{\Omega}{2}e^{-i\Delta t}(|1RR\rangle+|R1R\rangle+|RR1\rangle)\langle RRR|+\text{H.c.}\end{aligned} \tag{A6}$$

Traditionally, the dispersive coupling terms in the effective Hamiltonian should be discarded. Nevertheless, here we keep these terms temporarily to see whether they can induce some effective coupling under the higher-order perturbation theory. We use $\hat{P}'(\pm\Delta)_{\rm eff}^{(0-2)}$ and $\hat{P}''(\pm\Delta)_{a\Omega 3}$ to denote the terms of $\hat{H}_{\rm eff}^{(0-2)'}$ associated with $\Omega^2/(4\Delta)e^{\pm i\Delta t}$ and the terms of $\hat{H}''_{a\Omega 3}$ associated with $\Omega/2e^{\pm i\Delta t}$, respectively. Eventually, one can get the effective Hamiltonian as

$$\begin{aligned}\hat{H}_{\rm eff} &= \hat{H}_{\rm eff,part}^{(0-2)}+\frac{\Omega^4}{4\Delta^3}\{[\hat{P}'(\Delta)_{\rm eff}^{(0-2)},\hat{P}'(-\Delta)_{\rm eff}^{(0-2)}]\}\\ &\quad+\frac{\Omega^3}{4\Delta^2}\{[\hat{P}'(\Delta)_{\rm eff}^{(0-2)},\hat{P}''(-\Delta)_{a\Omega 3}]\\ &\quad+[\hat{P}''(\Delta)_{a\Omega 3},\hat{P}'(-\Delta)_{\rm eff}^{(0-2)}]\}\\ &\quad+\frac{\Omega^2}{4\Delta}\{[\hat{P}''(\Delta)_{a\Omega 3},\hat{P}''(-\Delta)_{a\Omega 3}]\}\\ &= \hat{H}_{\rm eff,part}^{(0-2)}+\frac{\Omega^4}{4\Delta^3}[|011\rangle\langle 011|+|101\rangle\langle 101|+|110\rangle\langle 110|\\ &\quad+3|111\rangle\langle 111|-(|0RR\rangle\langle 0RR|+|R0R\rangle\langle R0R|\\ &\quad+|RR0\rangle\langle RR0|+|1RR\rangle\langle 1RR|+|R1R\rangle\langle R1R|\\ &\quad+|RR1\rangle\langle RR1|)]+\frac{3\Omega^3}{4\Delta^2}(|111\rangle\langle RRR|+\text{H.c.})\\ &\quad+\frac{\Omega^2}{4\Delta}(|1RR\rangle\langle 1RR|+|R1R\rangle\langle R1R|\\ &\quad+|RR1\rangle\langle RR1|+3|RRR\rangle\langle RRR|).\end{aligned} \tag{A7}$$

By observing and analyzing the effective Hamiltonian, (A7), one can safely discard terms which include single- and two-Rydberg excitations since they are not included in the initial states and also do not couple with the zero- and three-excitation subspaces. In addition, the higher-order terms $\sim\Omega^4/\Delta^3$ can be discarded, in contrast to the terms $\sim\Omega^2/\Delta$ and Ω^3/Δ^2. Then Eq. (A7) is simplified to

$$\begin{aligned}\hat{H}_{\rm eff} &= \frac{\Omega^2}{4\Delta}[|100\rangle\langle 100|+|010\rangle\langle 010|+|001\rangle\langle 001|\\ &\quad+2(|110\rangle\langle 110|+|101\rangle\langle 101|+|011\rangle\langle 011|)\\ &\quad+3(|111\rangle\langle 111|+|RRR\rangle\langle RRR|)]\\ &\quad+\frac{3\Omega^3}{4\Delta^2}(|111\rangle\langle RRR|+\text{H.c.}).\end{aligned} \tag{A8}$$

Similarly to the above process, one can get the effective Hamiltonian relevant to ω as

$$\begin{aligned}\hat{H}_{\rm eff} &= -\frac{\omega^2}{4\delta}[|100\rangle\langle 100|+|010\rangle\langle 010|+|001\rangle\langle 001|\\ &\quad+2(|110\rangle\langle 110|+|101\rangle\langle 101|+|011\rangle\langle 011|)\\ &\quad+3|111\rangle\langle 111|].\end{aligned} \tag{A9}$$

Combining Eqs. (A8) and (A9), if the condition $\Omega^2/\Delta=\omega^2/\delta$ is satisfied, one can get the effective Hamiltonian of the whole system, as shown in Eq. (8).

2. Method 2

After performing the rotation operation with respect to $\hat{U}=e^{-i\hat{H}_v t}$, the total Hamiltonian relevant to Ω is $\hat{H}'_{a\Omega}=\hat{H}_{a\Omega 1}+\hat{H}_{a\Omega 2}+\hat{H}_{a\Omega 3}$, in which

$$\begin{aligned}\hat{H}_{a\Omega 1} &= \frac{\Omega}{2}e^{i\Delta t}(|100\rangle\langle R00|+|101\rangle\langle R01|+|110\rangle\langle R10|\\ &\quad+|111\rangle\langle R11|+|010\rangle\langle 0R0|+|011\rangle\langle 0R1|\\ &\quad+|110\rangle\langle 1R0|+|111\rangle\langle 1R1|+|001\rangle\langle 00R|\\ &\quad+|011\rangle\langle 01R|+|101\rangle\langle 10R|+|111\rangle\langle 11R|)+\text{H.c.},\\ \hat{H}_{a\Omega 2} &= \frac{\Omega}{2}(|10R\rangle\langle R0R|+|11R\rangle\langle R1R|+|1R0\rangle\langle RR0|\\ &\quad+|1R1\rangle\langle RR1|+|01R\rangle\langle 0RR|+|11R\rangle\langle 1RR|\\ &\quad+|R10\rangle\langle RR0|+|R11\rangle\langle RR1|+|0R1\rangle\langle 0RR|\\ &\quad+|1R1\rangle\langle 1RR|+|R01\rangle\langle R0R|+|R11\rangle\langle R1R|)\\ &\quad+\text{H.c.},\\ \hat{H}_{a\Omega 3} &= \frac{\Omega}{2}e^{-i\Delta t}(|1RR\rangle+|R1R\rangle+|RR1\rangle)\langle RRR|+\text{H.c.},\end{aligned} \tag{A10}$$

from which one can find that (i) the zero-excitation subspace couples to the one-excitation subspace with detuning $-\Delta$, (ii) the three-excitation subspace couples to the two-excitation subspace with the same detuning $-\Delta$, and (iii) the one- and two-excitation subspaces couple with each other resonantly.

Subsequently, based on the second-order perturbation theory, one can get

$$\begin{aligned}&\frac{|100\rangle\langle 100|\hat{H}'_{a\Omega}|R00\rangle\langle R00|\hat{H}'_{a\Omega}|100\rangle\langle 100|}{\Delta}=\frac{\Omega^2}{4\Delta}|100\rangle\langle 100|,\ \frac{|010\rangle\langle 010|\hat{H}'_{a\Omega}|0R0\rangle\langle 0R0|\hat{H}'_{a\Omega}|010\rangle\langle 010|}{\Delta}=\frac{\Omega^2}{4\Delta}|010\rangle\langle 010|,\\ &\frac{|001\rangle\langle 001|\hat{H}'_{a\Omega}|00R\rangle\langle 00R|\hat{H}'_{a\Omega}|001\rangle\langle 001|}{\Delta}=\frac{\Omega^2}{4\Delta}|001\rangle\langle 001|.\end{aligned} \tag{A11}$$

Besides, the Stark shifts relevant to $|110\rangle$ are calculated as

$$\frac{|110\rangle\langle 110|\hat{H}'_{a\Omega}|R10\rangle\langle R10|\hat{H}'_{a\Omega}|110\rangle\langle 110|}{\Delta}+\frac{|110\rangle\langle 110|\hat{H}'_{a\Omega}|1R0\rangle\langle 1R0|\hat{H}'_{a\Omega}|110\rangle\langle 110|}{\Delta}=\frac{\Omega^2}{2\Delta}|110\rangle\langle 110|,$$
$$\frac{|011\rangle\langle 011|\hat{H}'_{a\Omega}|0R1\rangle\langle 0R1|\hat{H}'_{a\Omega}|011\rangle\langle 011|}{\Delta}+\frac{|011\rangle\langle 011|\hat{H}'_{a\Omega}|01R\rangle\langle 01R|\hat{H}'_{a\Omega}|011\rangle\langle 011|}{\Delta}=\frac{\Omega^2}{2\Delta}|011\rangle\langle 011|,$$
$$\frac{|101\rangle\langle 101|\hat{H}'_{a\Omega}|R01\rangle\langle R01|\hat{H}'_{a\Omega}|101\rangle\langle 101|}{\Delta}+\frac{|101\rangle\langle 101|\hat{H}'_{a\Omega}|10R\rangle\langle 10R|\hat{H}'_{a\Omega}|101\rangle\langle 101|}{\Delta}=\frac{\Omega^2}{2\Delta}|101\rangle\langle 101|. \quad \text{(A12)}$$

Similarly, the Stark shifts relevant to $|011\rangle$ and $|101\rangle$ are also obtained as $\Omega^2/(2\Delta)|011\rangle\langle 011|$ and $\Omega^2/(2\Delta)|101\rangle\langle 101|$, respectively. And the Stark shift relevant to $|111\rangle$ is

$$\frac{|111\rangle\langle 111|\hat{H}'_{a\Omega}|R11\rangle\langle R11|\hat{H}'_{a\Omega}|111\rangle\langle 111|}{\Delta}+\frac{|111\rangle\langle 1R1|\hat{H}'_{a\Omega}|1R1\rangle\langle 1R1|\hat{H}'_{a\Omega}|111\rangle\langle 111|}{\Delta}$$
$$+\frac{|111\rangle\langle 11R|\hat{H}'_{a\Omega}|11R\rangle\langle 11R|\hat{H}'_{a\Omega}|111\rangle\langle 111|}{\Delta}=\frac{3\Omega^2}{4\Delta}|111\rangle\langle 111|. \quad \text{(A13)}$$

Similarly, one can get that the Stark shift related to state $|RRR\rangle$ is $3\Omega^2/(4\Delta)|RRR\rangle\langle RRR|$. Based on the third-order perturbation theory, one can get (The dynamics processes are shown in Fig. 2.)

$$\frac{|111\rangle\langle 111|\hat{H}'_{a\Omega}|R11\rangle\langle R11|\hat{H}'_{a\Omega}|RR1\rangle\langle RR1|\hat{H}'_{a\Omega}|RRR\rangle\langle RRR|}{\Delta^2}$$
$$+\frac{|111\rangle\langle 111|\hat{H}'_{a\Omega}|R11\rangle\langle R11|\hat{H}'_{a\Omega}|R1R\rangle\langle R1R|\hat{H}'_{a\Omega}|RRR\rangle\langle RRR|}{\Delta^2}$$
$$+\frac{|111\rangle\langle 111|\hat{H}'_{a\Omega}|1R1\rangle\langle 1R1|\hat{H}'_{a\Omega}|RR1\rangle\langle RR1|\hat{H}'_{a\Omega}|RRR\rangle\langle RRR|}{\Delta^2}$$
$$+\frac{|111\rangle\langle 111|\hat{H}'_{a\Omega}|1R1\rangle\langle 1R1|\hat{H}'_{a\Omega}|1RR\rangle\langle 1RR|\hat{H}'_{a\Omega}|RRR\rangle\langle RRR|}{\Delta^2}$$
$$+\frac{|111\rangle\langle 111|\hat{H}'_{a\Omega}|11R\rangle\langle 11R|\hat{H}'_{a\Omega}|R1R\rangle\langle R1R|\hat{H}'_{a\Omega}|RRR\rangle\langle RRR|}{\Delta^2}$$
$$+\frac{|111\rangle\langle 111|\hat{H}'_{a\Omega}|11R\rangle\langle 11R|\hat{H}'_{a\Omega}|1RR\rangle\langle 1RR|\hat{H}'_{a\Omega}|RRR\rangle\langle RRR|}{\Delta^2}$$
$$+\text{H.c.}=\frac{3\Omega^3}{4\Delta^2}|111\rangle\langle RRR|+\text{H.c.} \quad \text{(A14)}$$

After combining Eqs. (A11)–(A14), one can get the effective Hamiltonian, which is the same as that in Eq. (A8). In addition, using this method, one can get that the effective Hamiltonian relevant to ω is the same as that in Eq. (A9). Thus, if the condition $\Omega^2/\Delta=\omega^2/\delta$ is satisfied, one can get the effective Hamiltonian of the whole system, Eq. (8).

[1] T. F. Gallagher, *Rydberg Atoms* (Cambridge University Press, Cambridge, UK, 1994).

[2] M. Saffman, T. G. Walker, and K. Mølmer, Quantum information with Rydberg atoms, Rev. Mod. Phys. **82**, 2313 (2010).

[3] L. Béguin, A. Vernier, R. Chicireanu, T. Lahaye, and A. Browaeys, Direct Measurement of the Van Der Waals Interaction between Two Rydberg Atoms, Phys. Rev. Lett. **110**, 263201 (2013).

[4] D. Jaksch, J. I. Cirac, P. Zoller, S. L. Rolston, R. Côté, and M. D. Lukin, Fast Quantum Gates for Neutral Atoms, Phys. Rev. Lett. **85**, 2208 (2000).

[5] M. D. Lukin, M. Fleischhauer, R. Côté, L. M. Duan, D. Jaksch, J. I. Cirac, and P. Zoller, Dipole Blockade and Quantum Information Processing in Mesoscopic Atomic Ensembles, Phys. Rev. Lett. **87**, 037901 (2001).

[6] E. Urban, T. A. Johnson, T. Henage, L. Isenhower, D. D. Yavuz, T. G. Walker, and M. Saffman, Observation of Rydberg blockade between two atoms, Nat. Phys. **5**, 110 (2009).

[7] A. Gaëtan, Y. Miroshnychenko, T. Wilk, A. Chotia, M. Viteau, D. Comparat, P. Pillet, A. Browaeys, and P. Grangier, Observation of collective excitation of two individual atoms in the Rydberg blockade regime, Nat. Phys. **5**, 115 (2009).

[8] H. Busche, P. Huillery, S. W. Ball, T. Ilieva, M. P. A. Jones, and C. S. Adams, Contactless nonlinear optics mediated by long-range Rydberg interactions, Nat. Phys. **13**, 655 (2017).

[9] E. Brion, L. H. Pedersen, and K. Mølmer, Implementing a neutral atom Rydberg gate without populating the Rydberg state, J. Phys. B: At. Mol. Opt. Phys. **40**, S159 (2007).

[10] X.-F. Shi and T. A. B. Kennedy, Annulled van derWaals interaction and fast Rydberg quantum gates, Phys. Rev. A **95**, 043429 (2017).

[11] M. Müller, I. Lesanovsky, H. Weimer, H. P. Büchler, and P. Zoller, Mesoscopic Rydberg Gate Based on Electromagnetically Induced Transparency, Phys. Rev. Lett. **102**, 170502 (2009).

[12] L. Isenhower, E. Urban, X. L. Zhang, A. T. Gill, T. Henage, T. A. Johnson, T. G. Walker, and M. Saffman, Demonstration of a Neutral Atom Controlled-NOT Quantum Gate, Phys. Rev. Lett. **104**, 010503 (2010).

[13] E. Kuznetsova, T. Bragdon, R. Côté, and S. F. Yelin, Cluster-state generation using van der Waals and dipole-dipole interactions in optical lattices, Phys. Rev. A **85**, 012328 (2012).

[14] T. Xia, X. L. Zhang, and M. Saffman, Analysis of a controlled phase gate using circular Rydberg states, Phys. Rev. A **88**, 062337 (2013).

[15] M. H. Goerz, E. J. Halperin, J. M. Aytac, C. P. Koch, and K. B. Whaley, Robustness of high-fidelity Rydberg gates with single-site addressability, Phys. Rev. A **90**, 032329 (2014).

[16] D. D. Bhaktavatsala Rao and K. Mølmer, Robust Rydberg-interaction gates with adiabatic passage, Phys. Rev. A **89**, 030301(R) (2014).

[17] K. M. Maller, M. T. Lichtman, T. Xia, Y. Sun, M. J. Piotrowicz, A. W. Carr, L. Isenhower, and M. Saffman, Rydberg-blockade controlled-NOT gate and entanglement in a two-dimensional array of neutral-atom qubits, Phys. Rev. A **92**, 022336 (2015).

[18] S. Das, A. Grankin, I. Iakoupov, E. Brion, J. Borregaard, R. Boddeda, I. Usmani, A. Ourjoumtsev, P. Grangier, and A. S. Sørensen, Photonic controlled-PHASE gates through Rydberg blockade in optical cavities, Phys. Rev. A **93**, 040303(R) (2016).

[19] T. Keating, R. L. Cook, A. M. Hankin, Y.-Y. Jau, G. W. Biedermann, and I. H. Deutsch, Robust quantum logic in neutral atoms via adiabatic Rydberg dressing, Phys. Rev. A **91**, 012337 (2015).

[20] M. M. Müller, M. Murphy, S. Montangero, T. Calarco, P. Grangier, and A. Browaeys, Implementation of an experimentally feasible controlled-phase gate on two blockaded Rydberg atoms, Phys. Rev. A **89**, 032334 (2014).

[21] D. Petrosyan and K. Mølmer, Binding Potentials and Interaction Gates between Microwave-Dressed Rydberg Atoms, Phys. Rev. Lett. **113**, 123003 (2014).

[22] T. Keating, K. Goyal, Y.-Y. Jau, G. W. Biedermann, A. J. Landahl, and I. H. Deutsch, Adiabatic quantum computation with Rydberg-dressed atoms, Phys. Rev. A **87**, 052314 (2013).

[23] X. Q. Shao, D. X. Li, Y. Q. Ji, J. H. Wu, and X. X. Yi, Ground-state blockade of Rydberg atoms and application in entanglement generation, Phys. Rev. A **96**, 012328 (2017).

[24] X. F. Shi, Rydberg Quantum Gates Free From Blockade Error, Phys. Rev. Appl. **7**, 064017 (2017).

[25] D. Petrosyan, F. Motzoi, M. Saffman, and K. Mølmer, High-fidelity Rydberg quantum gate via a two-atom dark state, Phys. Rev. A **96**, 042306 (2017).

[26] I. I. Beterov and M. Saffman, Rydberg blockade, Förster resonances, and quantum state measurements with different atomic species, Phys. Rev. A **92**, 042710 (2015).

[27] T. Toffoli, in *Automata Languages and Programming, Seventh Colloquium*, Lectures Notes in Computer Science Vol. 84, edited by J. W. de Bakker and J. van Leeuwen (Springer, New York, 1980).

[28] E. Fredkin and T. Toffoli, Conservative logic, Int. J. Theor. Phys. **21**, 219 (1982).

[29] M. A. Nielsen and I. L. Chuang, *Quantum Computation and Quantum Information* (Cambridge University Press, Cambridge, UK, 2000).

[30] L. M. K. Vandersypen, M. Steffen, G. Breyta, C. S. Yannoni, M. H. Sherwood, and I. L. Chuang, Experimental realization of Shor's quantum factoring algorithm using nuclear magnetic resonance, Nature (London) **414**, 883 (2001).

[31] D. G. Cory, M. D. Price, W. Maas, E. Knill, R. Laflamme, W. H. Zurek, T. F. Havel, and S. S. Somaroo, Experimental Quantum Error Correction, Phys. Rev. Lett. **81**, 2152 (1998).

[32] M. Sarovar and G. J. Milburn, Continuous quantum error correction, in *Quantum Communication, Measurement and Computing*, edited by S. M. Barnett, O. Hirota, P. Öhberg, J. Jeffers, and E. Andersson, AIP Conf. Proc. No. 734 (AIP, New York, 2004), p. 121.

[33] A. Barenco, C. H. Bennett, R. Cleve, D. P. DiVincenzo, N. Margolus, P. Shor, T. Sleator, J. A. Smolin, and H. Weinfurter, Elementary gates for quantum computation, Phys. Rev. A **52**, 3457 (1995).

[34] M. Saeedi and M. Pedram, Linear-depth quantum circuits for n-qubit Toffoli gates with no ancilla, Phys. Rev. A **87**, 062318 (2013).

[35] S. B. Zheng, Implementation of Toffoli gates with a single asymmetric Heisenberg XY interaction, Phys. Rev. A **87**, 042318 (2013).

[36] E. Brion, A. S. Mouritzen, and K. Mølmer, Conditional dynamics induced by new configurations for Rydberg dipole-dipole interactions, Phys. Rev. A **76**, 022334 (2007).

[37] H. Z. Wu, Z. B. Yang, and S. B. Zheng, Implementation of a multiqubit quantum phase gate in a neutral atomic ensemble via the asymmetric Rydberg blockade, Phys. Rev. A **82**, 034307 (2010).

[38] L. Isenhower, M. Saffman, and K. Mølmer, Multibit C_k NOT quantum gates via Rydberg blockade, Quantum Inf. Process. **10**, 755 (2011).

[39] S. L. Su, Y. Gao, E. Liang, and S. Zhang, Fast Rydberg antiblockade regime and its applications in quantum logic gates, Phys. Rev. A **95**, 022319 (2017).

[40] C. Ates, T. Pohl, T. Pattard, and J. M. Rost, Antiblockade in Rydberg Excitation of an Ultracold Lattice Gas, Phys. Rev. Lett. **98**, 023002 (2007).

[41] T. Amthor, C. Giese, C. S. Hofmann, and M. Weidemüller, Evidence of Antiblockade in an Ultracold Rydberg Gas, Phys. Rev. Lett. **104**, 013001 (2010).

[42] T. Pohl and P. R. Berman, Breaking the Dipole Blockade: Nearly Resonant Dipole Interactions in Few-Atom Systems, Phys. Rev. Lett. **102**, 013004 (2009).

[43] J. Qian, Y. Qian, M. Ke, X. L. Feng, C. H. Oh, and Y. Z. Wang, Breakdown of the dipole blockade with a zero-area phase-jump pulse, Phys. Rev. A **80**, 053413 (2009).

[44] Z. C. Zuo and K. Nakagawa, Multiparticle entanglement in a one-dimensional optical lattice using Rydberg-atom interactions, Phys. Rev. A **82**, 062328 (2010).

[45] T. E. Lee, H. Häffner, and M. C. Cross, Collective Quantum Jumps of Rydberg Atoms, Phys. Rev. Lett. **108**, 023602 (2012).

[46] W. Li, C. Ates, and I. Lesanovsky, Nonadiabatic Motional Effects and Dissipative Blockade for Rydberg Atoms Excited From Optical Lattices or Microtraps, Phys. Rev. Lett. **110**, 213005 (2013).

[47] S. L. Su, E. J. Liang, S. Zhang, J. J. Wen, L. L. Sun, Z. Jin, and A. D. Zhu, One-step implementation of the Rydberg-Rydberg-interaction gate, Phys. Rev. A **93**, 012306 (2016).

[48] S. L. Su, Y. Z. Tian, H. Z. Shen, H. P. Zang, E. J. Liang, and S. Zhang, Applications of the modified Rydberg antiblockade regime with simultaneous driving, Phys. Rev. A **96**, 042335 (2017).

[49] A. W. Carr and M. Saffman, Preparation of Entangled and Antiferromagnetic States by Dissipative Rydberg Pumping, Phys. Rev. Lett. **111**, 033607 (2013).

[50] D. X. Li, X. Q. Shao, J. H. Wu, and X. X. Yi, Engineering steady-state entanglement via dissipation and quantum Zeno dynamics in an optical cavity, Opt. Lett. **42**, 3904 (2017); S. L. Su, Q. Guo, H. F. Wang, and S. Zhang, Simplified scheme for entanglement preparation with Rydberg pumping via dissipation, Phys. Rev. A **92**, 022328 (2015); X. Chen, H. Xie, G. W. Lin, X. Shang, M. Y. Ye, and X. M. Lin, Dissipative generation of a steady three-atom singlet state based on Rydberg pumping, *ibid.* **96**, 042308 (2017); X. Q. Shao, J. H. Wu, and X. X. Yi, Dissipation-based entanglement via quantum Zeno dynamics and Rydberg antiblockade, *ibid.* **95**, 062339 (2017); X. Q. Shao, J. H. Wu, X. X. Yi, and G. L. Long, Dissipative preparation of steady Greenberger-Horne-Zeilinger states for Rydberg atoms with quantum Zeno dynamics, *ibid.* **96**, 062315 (2017).

[51] I. I. Beterov, I. I. Ryabtsev, D. B. Tretyakov, and V. M. Entin, Quasiclassical calculations of blackbody-radiation-induced depopulation rates and effective lifetimes of Rydberg *nS*, *nP*, and *nD* alkali-metal atoms with $n \leqslant 80$, Phys. Rev. A **79**, 052504 (2009).

[52] L. D. Landau and E. M. Lifshitz, *Quantum Mechanics—Nonrelativistic Theory*, 3rd ed. (Elsevier Science, Oxford, UK, 1977).

[53] X. L. Zhang, L. Isenhower, A. T. Gill, T. G. Walker, and M. Saffman, Deterministic entanglement of two neutral atoms via Rydberg blockade, Phys. Rev. A **82**, 030306(R) (2010).

[54] S. de Léséleuc, D. Barredo, V. Lienhard, A. Browaeys, and T. Lahaye, Analysis of imperfections in the coherent optical excitation of single atoms to Rydberg states, Phys. Rev. A **97**, 053803 (2018).

[55] Y. Y. Jau, A. M. Hankin, T. Keating, I. H. Deutsch, and G. W. Biedermann, Entangling atomic spins with a Rydberg-dressed spin-flip blockade, Nat. Phys. **12**, 71 (2016).

[56] O. Gamel and D. F. V. James, Time-averaged quantum dynamics and the validity of the effective Hamiltonian model, Phys. Rev. A **82**, 052106 (2010).